

# Colon-Bench: An Agentic Workflow for Scalable Dense Lesion Annotation in Full-Procedure Colonoscopy Videos

Abdullah Hamdi, Changchun Yang, and Xin Gao

King Abdullah University of Science and Technology (KAUST)  
{abdullah.hamdi@kaust.edu.sa}

**Abstract.** Early screening via colonoscopy is critical for colon cancer prevention, yet developing robust AI systems for this domain is hindered by the lack of densely annotated, long-sequence video datasets. Existing datasets predominantly focus on single-class polyp detection and lack the rich spatial, temporal, and linguistic annotations required to evaluate modern Multimodal Large Language Models (MLLMs). To address this critical gap, we introduce Colon-Bench, generated via a novel multi-stage agentic workflow. Our pipeline seamlessly integrates temporal proposals, bounding-box tracking, AI-driven visual confirmation, and human-in-the-loop review to scalably annotate full-procedure videos. The resulting verified benchmark is unprecedented in scope, encompassing 528 videos, 14 distinct lesion categories (including polyps, ulcers, and bleeding), over 300,000 bounding boxes, 213,000 segmentation masks, and 133,000 words of clinical descriptions. We utilize Colon-Bench to rigorously evaluate state-of-the-art MLLMs across lesion classification, Open-Vocabulary Video Object Segmentation (OV-VOS), and video Visual Question Answering (VQA). The MLLM results demonstrate surprisingly high localization performance in medical domains compared to SAM-3. Finally, we analyze common VQA errors from MLLMs to introduce a novel "colon-skill" prompting strategy, improving zero-shot MLLM performance by up to 9.7% across most MLLMs. The dataset and the code are available at <https://abdullahamdi.com/colon-bench>

**Keywords:** colonoscopy · lesion detection · polyps · MLLMs.

## 1 Introduction

Colon cancer is the second leading cause of cancer death worldwide [23], and many of these deaths are preventable with early screening and removal of precancerous lesions; however, colonoscopy remains expensive, invasive, and logistically difficult to arrange, requiring specialized clinicians and often long procedures (up to two hours) that increase facility and staffing costs. Automated AI analysis promises to ease these burdens, but lesion discovery is a needle-in-a-haystack problem: lesions are sparse and frequently obscured by motion blur, occlusion,

**Table 1. Comparison of Colonoscopy Datasets.** Relative to prior datasets that emphasize single-class polyp detection or anatomical segmentation, *Colon-Bench* provides a broader lesion taxonomy and richer supervision. It combines long-sequence coverage with dense boxes, masks, and clinical text, enabling multi-task evaluation across detection, video segmentation, and language-based understanding.

Attribute	Kvasir-SEG [14]	SUN [19]	PolypGen [1]	REAL-Col. [3]	CAS-Col. [22]	Colon-Bench (Ours)
Year	2020	2021	2023	2024	2025	2026
Focus	Segmentation	Detection	Segmentation	Detection	Anatomy	<b>Lesion, Video Seg., &amp; Text</b>
Number of Videos	N/A	N/A	N/A	60	78	<b>528</b>
Total Frames/Images	1,000	158,690	6,282	<b>2,757,723</b>	1,961,100	464,035
Lesion Classes	1 (Polyp)	1 (Polyp)	1 (Polyp)	1 (Polyp)	N/A	<b>14 (Bleeding, Polyps, ...)</b>
Bounding Boxes	N/A	158,690	6,282	<b>351,264</b>	N/A	300,132
Segmentation Masks	1,000	N/A	6,282	N/A	Yes	<b>213,067</b>
Language Descriptions	N/A	N/A	N/A	N/A	N/A	<b>Yes (133k Words)</b>

debris, stool, or fluids, and by camera contact with the colon wall, making dense visual analysis challenging. Moreover, manual dense annotation of colonoscopy videos is labor-intensive and inconsistent, which motivates our work on a scalable, affordable pipeline for dense colonoscopy video annotation, facilitating AI research, evaluation, and applications in colonoscopy.

To address the inherent visual challenges of colonoscopy videos, recent methods have proposed specialized architectures optimized for pixel-level precision and subtle lesion identification [27,17]. Furthermore, because colonoscopy procedures are inherently long, efficient spatiotemporal analysis is critical; approaches utilizing state-space models [24] and token merging [26] have been introduced to capture long-range dependencies while reducing computational redundancy. Many methods rely on self-supervised learning with large-scale pretraining [15] or utilize a small number of annotated image examples with text [13], bounding boxes [7,16], or segmentation masks [14,7]. These architectural and synthetic workarounds underscore the critical gap in the field that our work addresses: the need for a comprehensive, densely annotated, long-sequence dataset to ground the spatiotemporal analysis of real colonoscopies.

REAL-COLON [3] introduced 60 long sequences of colonoscopy procedures. These colonoscopies are labeled with 351,264 bounding boxes on polyps using commercial software. CAS-COLON [22] introduced a colonoscopy anatomical temporal classification (which part of the colon is each image) with a total of 78 videos totaling 9 hours and around 2 million images. Other colonoscopy datasets are either small in size for comprehensive training and evaluations [18], or they cover large image datasets but are limited in the scope of tasks and types of lesions that they investigate [14,19,18,1]. As Table 1 shows, our Colon-Bench offers a dense annotation scheme for lesions (with text descriptions and segmentation mask tracklets) across a large variety of video clips and provides comprehensive evaluation benchmarks (including Video Question Answering, lesion clip classification, and Open-Vocabulary Video Segmentation) for MLLMs as a general tool for colonoscopy video understanding.

The rapid evolution of Large Language Models (LLMs) [20,11] and foundational vision-language models [21] has driven the development of Multimodal Large Language Models (MLLMs) capable of complex visual reasoning

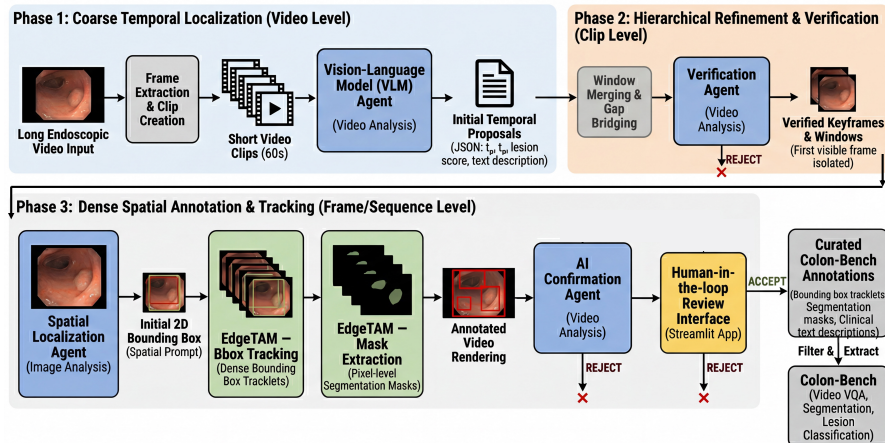


**Fig. 1. Colon-Bench Annotation Pipeline.** Overview of the multi-stage agentic workflow used to build the dataset, from VLM proposal generation through verification, tracking with spatial annotations, AI confirmation, and clinician review. The figure highlights how successive filters reduce false positives while adding dense spatial and textual labels for the retained windows, all easily verified by a physician at the end. The accepted annotations are then used to create a comprehensive Colon-Bench for MLLMs covering multiple video tasks: Visual Question Answering (VQA), binary lesion classification, and Open-Vocabulary Video Object Segmentation (OV-VOS).

[2,8,10,12,11]. While these MLLMs demonstrate remarkable zero-shot comprehension in general domains, their proficiency in interpreting long, occluded, and highly noisy medical sequences remains largely untested. This underscores the critical need for our proposed *Colon-Bench* to systematically evaluate how well these advanced video-language models understand complex colonoscopy procedures. Recent works show strong results with agentic MLLM pipelines for long-form videos [9,25] and for hybrid automatic labeling with human verification for large medical image datasets [6], motivating our pipeline in Fig. 1.

We provide a new annotated dataset of long sequences with dense annotations. It includes the first Open-Vocabulary Video Object Segmentation (OV-VOS) dataset in colonoscopy that involves mask tracking of lesions even with occluding frames. Our contributions can be summarized as follows:

**Contributions:** (i) We introduce a novel, multi-stage agentic workflow for the dense annotation of full-procedure colonoscopy videos. By combining temporal proposals, bounding-box tracking, AI-driven confirmation with visual cues, and an efficient human-in-the-loop review interface, our pipeline dramatically reduces manual labor while yielding high-quality spatial, temporal, and textual annotations. (ii) We present a comprehensive, multi-task video benchmark (*Colon-Bench*) for colonoscopy understanding. Spanning 14 distinct lesion categories (including polyps, bleeding, and ulcers), the dataset comprises over 464k frames, 300k bounding boxes, 213k segmentation masks, and 133k words of

**Table 2. Annotation Pipeline Stages.** We show Colon-Bench annotations after each major processing stage. As automated filters and human review progressively discard false-positive windows (reducing total frames), the temporal precision, F1 score, and specificity of the automatically identified lesions demonstrably increase on the surrogate polyp labels of REAL-COLON [3] (polyps are one type of lesion in Colon-Bench).

Metric	Initial VLM Proposals	+ verification Agent Filtering	+ Cued AI Confirmation Agent	Final Human-Curated Annots.
Total Windows	1,325	903	597	<b>528</b>
Total Frames	826,763	648,440	492,606	<b>464,035</b>
Duration (Hours)	22.97	18.01	13.68	<b>12.89</b>
Total Bounding Boxes	-	-	314,408	<b>300,132</b>
Total Seg. Masks	-	-	227,343	<b>213,067</b>
Total Clinical Words	-	-	145,515	<b>133,289</b>
Precision	30.9	36.2	53.1	<b>55.4</b>
Recall	67.5	68.7	48.8	<b>48.6</b>
F1 Score	42.4	47.4	50.8	<b>51.8</b>
Specificity	78.6	82.9	93.9	<b>94.4</b>

clinical descriptions, all verified by humans and an experienced surgeon. It facilitates four rigorous evaluation tasks: binary lesion classification, Open-Vocabulary Video Object Segmentation (OV-VOS), and two difficulty tiers of Video Visual Question Answering (VQA). **(iii)** We conduct a large-scale evaluation of colonoscopy visual reasoning and localization in state-of-the-art MLLMs (e.g., Gemini 3, Qwen, Seed, GPT), focused on lesions. By analyzing error patterns across MLLMs, we propose a novel “colon-skill” that distills cross-model error patterns into structured textual guidance, which we show improves most MLLM performance by up to 9.7% without any additional training (only adding the text skill to the prompt improves performance).

## 2 Methodology

### 2.1 Agentic Workflow for Colonoscopy Annotation

**Automatic annotations with quality control.** As illustrated in Fig. 1, our dense colonoscopy annotations were constructed by applying a multi-stage agentic pipeline to 60 video sequences from the REAL-COLON dataset [3]. As detailed in Table 2, an initial vision-language model identified 1,325 candidate lesion windows (22.97 hours). Successive verification filtering agent, bounding-box tracking, cued AI confirmation agent (using an overlay of the box on the lesion as cues), and a final human review progressively filtered this set to isolate high-quality detections. By observing the dataset state at each stage (Table 2), we demonstrate that automated AI stages provide the principal filtering gains on the surrogate polyp labels of REAL-COLON [3] (polyps are one type of lesion in Colon-Bench, but act as a quality control). Initial video verification followed by EdgeTAM [28] tracking (efficient SAM-based tracking and segmentation) and AI confirmation simultaneously established the spatial annotations (yielding over 314k initial bounding boxes) and radically pruned weak temporal boundaries. The recent

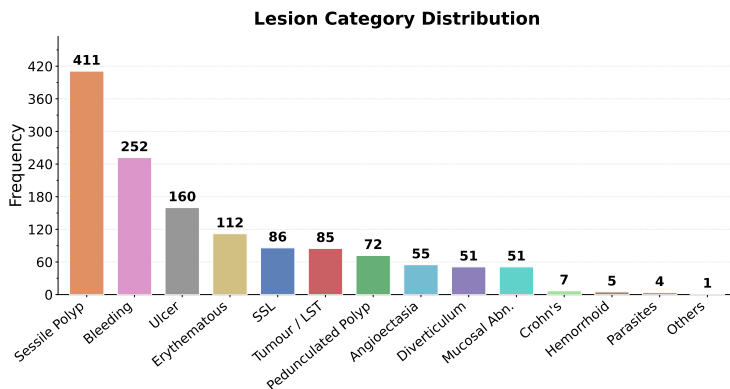


**Fig. 2. Lesion Category Distribution.** Long-tailed lesion category distribution in Colon-Bench, highlighting the diversity of lesions.

success of the Gemini-3 vision model for medical domains [4] has prompted the use of Gemini-3 as one tool in the annotation pipeline. For proposals, video verification agents, and bounding boxes, Gemini-2.5-flash-lite, Gemini-3-pro, and Gemini-3-flash were used, respectively, balancing performance and cost (Table 3).

**Human review.** Human review served as the final quality gate. To enable efficient review at scale, the pipeline pre-rendered short clips with spatial overlays into an interactive web interface. A reviewing physician rejected only 69 of the 597 presented windows (11.6%), demonstrating strong agreement with the AI filters. Ultimately, the pipeline retained 528 curated windows (39.8% retention) spanning 464,035 frames. The final dataset yields a dense, multi-modal benchmark comprising 300,132 bounding boxes, 213,067 segmentation masks, and over 133k words of verified clinical text (averaging 252.4 words per window).

**Lesion types.** The dataset spans 14 lesion categories identified through multi-label keyword matching over clinician-verified text fields (Fig. 2). The distribution is heavily long-tailed: sessile polyps dominate (411 windows), followed by bleeding (252), ulcers (160), and erythematous lesions (112). Because Colon-bench descriptions are free-form text (one window can have multiple lesions), a single review window may contribute to more than one category.

## 2.2 Colon-Bench Evaluation Benchmark

**Filtering.** Colon-Bench is a multi-task video benchmark for colonoscopy understanding comprising 1,597 clips from 60 patients (955,126 frames), spanning five tasks: binary classification (790 clips), detection (272 clips, 61,538 per-frame bounding boxes), instance segmentation (264 clips, 57,550 per-frame masks), and VQA at two difficulty tiers. The binary lesion classes and segmentation masks follow directly from Sec. 2.1 to establish the first colonoscopy Open-Vocabulary Video Object Segmentation (OV-VOS) benchmark.

**VQA (prompted & unprompted)** . The *prompted* VQA split contains 1,485 five-choice questions over 499 clips whose videos include bounding-box overlays

**Table 3. Colon-Bench Combined Results.** Summary of model performance across the four benchmark tasks: visual prompted and unprompted video Visual Question Answering (VQA) accuracy (with visual box prompts and without them), binary lesion classification precision/recall/F1, and open-vocabulary video segmentation IoU/Dice. The video segmentation is based on 3 box detections for each MLLM prompting the same EdgeTAM tracker [28]. Best scores per metric are shown in **bold**.

Model	VQA Accuracy		Lesion Cls.			Segmentation	
	Prompted	Unprompted	Precision	Recall	F1	IoU	Dice
CLIP [21]	-	-	34.5	<b>100</b>	51.3	-	-
ViCLIP [25]	-	-	34.8	98.5	51.4	-	-
Endo-CLIP [13]	-	-	41.9	95.2	58.2	-	-
Colon-ViCLIP [25]	-	-	49.0	84.2	62.0	-	-
SAM 3 [5]	-	-	-	-	-	2.5	2.9
GPT-4o	-	-	-	-	-	0.5	0.8
Claude Opus 4.6	-	-	-	-	-	16.1	20.5
GPT-5.2	-	-	-	-	-	30.7	36.5
GPT-5.4	-	-	-	-	-	34.5	41.1
Qwen3-VL 8B	32.9	38.3	34.4	<b>100</b>	51.2	10.4	13.1
Seed 1.6 Flash	38.1	45.4	<b>94.2</b>	24.3	38.6	2.6	3.5
Qwen-VL Max	39.1	45.4	0.0	0.0	0.0	25.6	29.6
Qwen3-VL 32B	39.3	44.4	0.0	0.0	0.0	12.7	15.9
Qwen3.5 Plus	44.3	60.5	36.2	24.6	29.3	16.7	21.0
Molmo 2-8B	46.1	53.4	52.9	46.7	49.6	2.6	3.8
Qwen3-VL 235B	46.7	56.6	22.2	0.7	1.4	13.6	16.9
Gemini 2.5 F. Li.	47.8	46.8	42.3	95.9	58.7	19.9	24.3
Qwen3.5 397B	49.0	60.1	10.0	0.4	0.7	16.6	21.0
GLM-4.6V	55.7	53.8	46.5	94.1	62.2	12.5	16.1
Seed 1.6	62.9	72.0	85.0	58.7	69.4	12.6	16.1
Gemini 3.1 F. Li.	69.2	67.7	72.6	90.8	<b>80.7</b>	37.4	43.4
Gemini 3 Flash	76.6	76.0	55.3	97.1	70.5	<b>48.3</b>	<b>54.7</b>
Gemini 3 Pro	<b>78.6</b>	<b>82.5</b>	66.1	93.0	77.3	45.0	51.3

on confirmed lesion windows; the *unprompted* split contains 2,740 questions over 918 clips rendered from raw frames, fully encompassing all detection and segmentation videos. For instance, an unprompted question for the clip in Fig. 3 first row asks: “How is the morphology and anatomical location of the identified lesion described?” with distractors spanning pedunculated, depressed, and flat lesions at various anatomical sites; the correct answer is (D) a sessile polyp on a haustral fold. More examples are shown in the Appendix.

**Debiasing Colon-Bench.** For each clip, three five-way MCQs are generated with Gemini-3, covering lesion identification, clinical characteristics, and temporal reasoning. To mitigate text-only shortcuts, we apply two-stage debiasing: (i) adversarial distractors are regenerated in a separate LLM call receiving only the stem and correct answer; (ii) a blind text-only stress-test identifies and reverts any newly introduced bias. Post-debiasing blind accuracy is 44.6% (prompted) and 37.1% (unprompted) vs. the 20% random baseline, with residual margins reflecting dataset priors rather than surface cues.

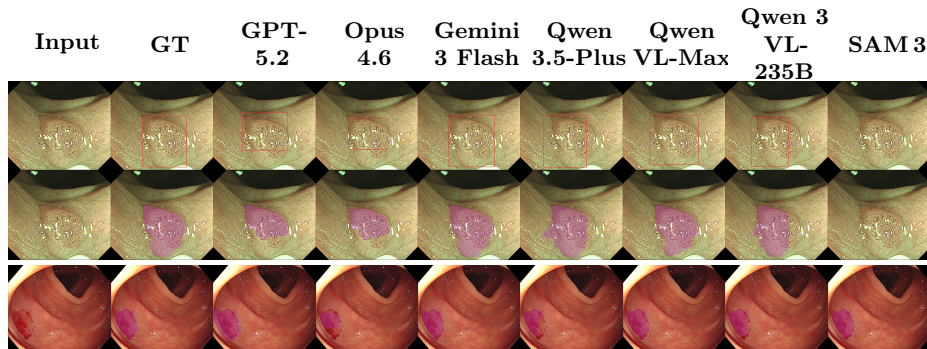


**Fig. 3. Qualitative Comparisons.** The first row shows detection (*Sessile Polyp*); the remaining rows show segmentation (*Sessile Polyp & Erythematous Region*). Columns show the input, ground truth, and model outputs. SAM-3 underperforms compared to modern MLLMs when paired with a prompted tracker such as EdgeTAM [28].

**Baselines.** Methods reported in this work include a set of Multimodal Large Language Models (MLLMs) such as different variants of GPTs, Gemini, Qwen, Seed, GLM, and Molmo [20,2,8,10,12,11]. Also we report (for some corresponding benchmarks) SAM-3 [5], CLIP [21], Video CLIP (ViCLIP) [25] and its fine-tuned version on Colon-Bench text (Colon-CLIP), and a recent model Endo-CLIP [13]. Models that do not have video API support (*E.g.* GPT-series) are only evaluated on the segmentation task. All models in segmentation (Except SAM-3) are based on 3-frame box detections prompting EdgeTAM tracker [28].

### 2.3 Colon-Bench Results

Table 3 reveals a clear performance hierarchy across all four Colon-Bench tasks. Gemini 3 Pro and Gemini 3 Flash consistently dominate, achieving the highest VQA accuracy on both prompted and unprompted splits and the best segmentation quality (IoU/Dice of 45-48%/51-55%), while Gemini 3.1 Flash Lite leads in classification F1 (80.7%). Among open-weight models, Seed 1.6 is the strongest overall, ranking third in VQA and delivering competitive classification F1 (69.4%) with the highest precision among full-benchmark models (85.0%). The Qwen family shows mixed behavior: larger variants (Qwen3.5 397B, Qwen3-VL 235B) perform well on VQA yet nearly collapse on classification ( $R < 1\%$ ,  $F1 < 2\%$ ), suggesting they default to the majority (negative) benign class rather than detecting lesion presence. For segmentation, performance drops sharply beyond the top three models. Overall, our Colon-Bench demonstrates how these strong MLLM models can be used for lesion detection in short clips, beating specialized models like Endo-CLIP [13] by 30%. For the task of open-vocabulary lesion segmentation in video clips, an MLLM like GPT-5.4 (when combined with box-promptable EdgeTAM tracker [28]) beats SAM-3 [5] by 32.0% mIoU (see Fig. 4).

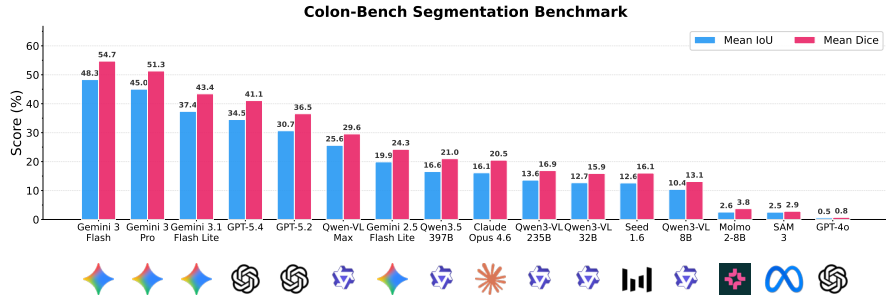


**Fig. 4. Multi-Modal Large Language Models for Lesion Segmentation.** Video object segmentation results on the 272-video benchmark, where MLLMs [20,2,8,10,12,11] first localize the target lesion with 3 bounding boxes and a EdgeTAM tracker [28] propagates masks.

### 3 Analysis and Insights

#### 3.1 Colon-Skill for MLLMs

To test whether Multimodal Large Language Models (MLLMs) benefit from structured domain knowledge at inference time, we use a two-stage skill-extraction and prompt-augmentation pipeline. First, we collect per-model VQA predictions on the full benchmark and stratify errors by lesion category (Fig. 2), retaining only questions that a majority of models answer incorrectly. These shared failure cases, along with their question/answer context and category metadata, are fed to a frontier large language model which synthesises a concise, natural-language *Colon-Skill*: morphological cues, common confusion traps, and a decision checklist tailored to colonoscopic VQA. Second, we prepend this Colon-Skill to every VQA prompt and re-evaluate all models under identical conditions, yielding consistent improvements up to +9.7% (Fig. 5). This suggests that distilling cross-model error patterns into structured textual guidance is an effective, training-free way to improve MLLM performance on specialised medical VQA tasks, particularly when models can integrate the added context.

#### 3.2 Ablation Study

**Effect of frame count on segmentation.** As shown in Fig. 6, increasing the number of input frames for detection yields steady gains in downstream segmentation quality. For instance, expanding the context from 1 to 7 frames boosts the mean IoU of Gemini 3 Flash from 43.1% to 54.4% (mDice: 48.8% to 61.5%), and similarly improves Qwen-VL Max from 19.7% to 33.7% mIoU. However, this comes with a significant cost as these are per-window detections. We pick 3 equally-spaced frames per window as a good trade-off in all of our segmentation results in this work.

**Temporal context in VQA.** Evaluating temporal context on the prompted VQA split showed that full video generally outperforms single-frame inputs,

though the degree of impact is model-dependent. Restricting the input to a single frame reduced accuracy for Qwen3.5 397B (-7.0%), Qwen-VL Max (-3.4%), and Gemini 3 Flash (-2.5%). This highlights the importance of using videos instead of images used in previous polyp detection benchmarks.

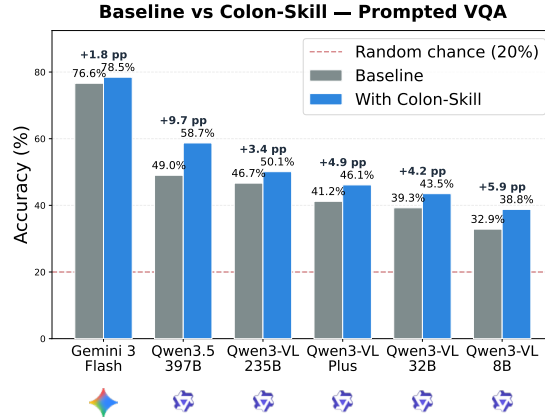


**Fig. 5. Colon-Skill on Prompted VQA.** Skill-augmented prompting on the prompted VQA split, where a distilled error-based skill context yields consistent accuracy improvements for higher-capacity models.

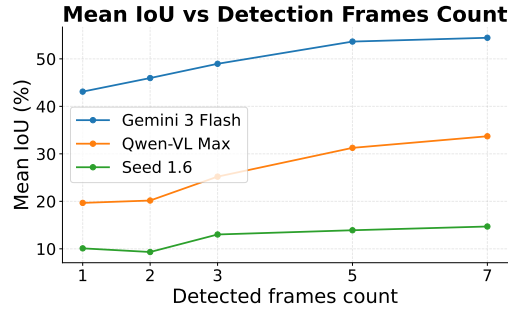


**Fig. 6. Ablation Study on Lesion Segmentation.** We ablate the number of detection frames per window used in the segmentation benchmark, showing diminishing improvement in downstream segmentation quality.

## 4 Conclusions

We presented Colon-Bench, a novel agentic workflow and a comprehensive multi-task benchmark for full-procedure colonoscopy video understanding. By scalably

and densely annotating 14 distinct lesion categories with masks, bounding boxes, and clinical text, we demonstrated that state-of-the-art MLLMs excel at high-level colonoscopy reasoning and spatial grounding with engineered context and agentic workflows. Future work will focus on optimizing these agent-driven pipelines for real-time deployment in clinical settings, lowering the barrier to affordable and accurate colon cancer screening.

**Acknowledgments.** We thank Dr. Jamal Hamdi, a surgeon with over 30 years of experience, who reviewed the accuracy of the Colon-Bench annotations together with the authors. This work was supported by the King Abdullah University of Science and Technology (KAUST) Center of Excellence for Smart Health. Additional support came from the KAUST Ibn Rushd Postdoctoral Fellowship Program.

**License.** Colon-Bench is intended strictly for academic research, and any form of commercial use is prohibited. Copyright for all videos is retained by their owners [3]. The dataset as a whole is licensed under the Creative Commons Attribution (CC BY) license, consistent with the licensing of the original REAL-COLON dataset [3].

## References

1. Ali, S., Jha, D., Ghatwary, N., Realdon, S., Cannizzaro, R., Salem, O.E., Lamarão, D.V., Da Roza, C., Riegler, M.A., Halvorsen, P.: A multi-centre polyp detection and segmentation dataset for generalisability assessment. *Scientific Data* **10**(1), 75 (2023) [2](#)
2. Bai, S., Cai, Y., Chen, R., Chen, K., Chen, X., Cheng, Z., Deng, L., Ding, W., Gao, C., Ge, C., et al.: Qwen3-vl technical report. arXiv preprint arXiv:2511.21631 (2025) [3](#), [7](#), [8](#)
3. Biffi, C., Antonelli, G., Bernhofer, S., Hassan, C., Hirata, D., Iwatate, M., Maieron, A., Salvagnini, P., Cherubini, A.: Real-colon: A dataset for developing real-world ai applications in colonoscopy. *Scientific Data* **11**(1), 539 (2024). <https://doi.org/10.1038/s41597-024-03359-0> [2](#), [4](#), [10](#), [13](#), [16](#)
4. Bose, K., Kumar, A., Soundararajan, R., Mudgil, P., Ralmilay, S., Dutta, N., Singhal, M., Kumar, A., Sen, S., Patra, A., et al.: Multi-rads synthetic radiology report dataset and head-to-head benchmarking of 41 open-weight and proprietary language models. arXiv preprint arXiv:2601.03232 (2026) [5](#)
5. Carion, N., Gustafson, L., Hu, Y.T., Debnath, S., Hu, R., Suris, D., Ryali, C., Alwala, K.V., Khedr, H., Huang, A., et al.: Sam 3: Segment anything with concepts. arXiv preprint arXiv:2511.16719 (2025) [6](#), [7](#)
6. Chambon, P., Delbrouck, J.B., Sounack, T., Huang, S.C., Chen, Z., Varma, M., Truong, S.Q., Chuong, C.T., Langlotz, C.P.: Chexpert plus: Augmenting a large chest x-ray dataset with text radiology reports, patient demographics and additional image formats. arXiv preprint arXiv:2405.19538 (2024) [3](#)
7. Choudhuri, A., Gao, Z., Zheng, M., Planche, B., Chen, T., Wu, Z.: Polypseg-track: Unified foundation model for colonoscopy video analysis. In: *Medical Image Computing and Computer Assisted Intervention – MICCAI 2025*. Springer (2025) [2](#)
8. Deitke, M., Clark, C., et al.: Molmo and pixmo: Open weights and open data for state-of-the-art vision-language models. In: *Proceedings of the IEEE/CVF Conference on Computer Vision and Pattern Recognition (CVPR)* (2025) [3](#), [7](#), [8](#)

9. Fan, Y., Ma, X., Wu, R., Du, Y., Li, J., Gao, Z., Li, Q.: Videoagent: A memory-augmented multimodal agent for video understanding. In: European Conference on Computer Vision. pp. 75–92. Springer (2024) 3
10. Ge, Y., Zhao, Y., Zhu, Z., et al.: Planting a seed of vision in large language model. arXiv preprint arXiv:2307.08041 (2023) 3, 7, 8
11. Gemini Team: Gemini 1.5: Unlocking multimodal understanding across millions of tokens of context. arXiv preprint arXiv:2403.05530 (2024) 2, 3, 7, 8
12. GLM Team: Glm-4: Open multilingual multimodal chat lms (2024), <https://github.com/THUDM/GLM-4> 3, 7, 8
13. He, Y., Zhu, Y., Fu, P., Yang, R., Chen, T., Wang, Z., Li, Q., Zhou, P., Yang, X., Wang, S.: Endo-clip: Progressive self-supervised pre-training on raw colonoscopy records. In: Medical Image Computing and Computer Assisted Intervention – MICCAI 2025. Springer (2025), early accepted. Available at: <https://arxiv.org/abs/2505.09435> 2, 6, 7
14. Jha, D., Smedsrud, P.H., Riegler, M.A., Halvorsen, P., de Lange, T., Johansen, D., Johansen, H.D.: Kvasir-seg: A segmented polyp dataset. In: MultiMedia Modeling. Lecture Notes in Computer Science, vol. 11962, pp. 451–462. Springer, Cham (2020). [https://doi.org/10.1007/978-3-030-37734-2\\_37](https://doi.org/10.1007/978-3-030-37734-2_37) 2
15. Jong, M.R., Boers, T.G.W., Kusters, K.H.J., Jaspers, T.J.M., van der Putten, J.A., de With, P.H.N., van der Sommen, F., de Groof, A.J., Bergman, J.J.G.H.M., et al.: Gastronet-5m: A multicenter dataset for developing foundation models in gastrointestinal endoscopy. *Gastroenterology* **170**(1), 174–187 (2026). <https://doi.org/10.1053/j.gastro.2025.07.030> 2
16. Li, K., Fathan, M.I., Patel, K., Zhang, T., Zhong, C., Bansal, A., Rastogi, A., Wang, Z., Wang, G.: Colonoscopy polyp detection and classification: Dataset creation and comparative evaluations. *PLoS ONE* **16**(8), e0255809 (2021) 2
17. Li, S., Ren, Y., Yu, Y., Li, H.: A survey of deep learning algorithms for colorectal polyp segmentation. *Neurocomputing* (2024) 2
18. Ma, Y., Chen, X., Cheng, K., Li, Y., Sun, B.: Ldpolypvideo benchmark: A large-scale colonoscopy video dataset of diverse polyps. In: Medical Image Computing and Computer Assisted Intervention–MICCAI 2021: 24th International Conference. pp. 387–396. Springer (2021) 2
19. Misawa, M., Kudo, S.e., Mori, Y., Maeda, Y., Kataoka, S., Ogata, N., Ichimasa, K., Kudo, T., Mori, K., Ishigaki, T.: Development of a computer-aided detection system for colonoscopy and a publicly accessible large colonoscopy video database (with video). *Gastrointestinal Endoscopy* **93**(4), 960–967 (2021) 2
20. OpenAI: Gpt-4 technical report (2023) 2, 7, 8
21. Radford, A., Kim, J.W., Hallacy, C., Ramesh, A., Goh, G., Agarwal, S., Sastry, G., Askell, A., Mishkin, P., Clark, J., et al.: Learning transferable visual models from natural language supervision. In: ICML. pp. 8748–8763. PMLR (2021) 2, 6, 7
22. Song, Y., Zhang, Z., Wang, R., Zhong, L., Cai, C., Chen, J., Zhou, Y., Wang, X., Li, Z., Yang, L., Li, Z., Yan, H., Zhang, Q., Qian, D., Li, X.: Cas-colon: A comprehensive colonoscopy anatomical segmentation dataset for artificial intelligence development. *Scientific Data* **12**(1), 1382 (2025). <https://doi.org/10.1038/s41597-025-05588-3> 2
23. Sung, H., Ferlay, J., Siegel, R.L., Laversanne, M., Soerjomataram, I., Jemal, A., Bray, F.: Global cancer statistics 2020: Globocan estimates of incidence and mortality worldwide for 36 cancers in 185 countries. *CA: A Cancer Journal for Clinicians* **71**(3), 209–249 (2021). <https://doi.org/10.3322/caac.21660> 1
24. Tian, Q., Liao, H., Huang, X., Yang, B., Lei, D., Ourselin, S., Liu, H.: Endomamba: An efficient foundation model for endoscopic videos via hierarchical pre-training. In:

- Medical Image Computing and Computer Assisted Intervention – MICCAI 2025. Springer (2025) [2](#)
25. Wang, Y., He, Y., Li, Y., Li, K., Yu, J., Ma, X., Li, X., Chen, G., Chen, X., Wang, Y., Luo, P., Liu, Z., Wang, Y., Wang, L., Qiao, Y.: Internvid: A large-scale video-text dataset for multimodal understanding and generation. In: The Twelfth International Conference on Learning Representations (ICLR). OpenReview.net (2024), <https://openreview.net/forum?id=MLBdiWu4Fw> [3](#), [6](#), [7](#)
  26. Wang, Z., Liu, C., Dou, Q., Zhang, S., et al.: Improving foundation model for endoscopy video analysis via representation learning on long sequences. *IEEE Journal of Biomedical and Health Informatics* pp. 3526–3536 (2025). <https://doi.org/10.1109/JBHI.2025.3349925> [2](#)
  27. Zeng, Q., Xie, Y., Lu, Z., Lu, M., Wu, Y., Xia, Y.: Segment together: A versatile paradigm for semi-supervised medical image segmentation. *IEEE Transactions on Medical Imaging* **44**(7), 2948–2959 (2025). <https://doi.org/10.1109/TMI.2025.3360447> [2](#)
  28. Zhou, C., Zhu, C., Xiong, Y., Suri, S., Xiao, F., Wu, L., Krishnamoorthi, R., Dai, B., Loy, C.C., Chandra, V., et al.: Edgetam: On-device track anything model. In: Proceedings of the Computer Vision and Pattern Recognition Conference. pp. 13832–13842 (2025) [4](#), [6](#), [7](#), [8](#), [22](#)

## A Additional Dataset Details

### A.1 Annotation Pipeline

The benchmark was constructed through a multi-stage filtering pipeline applied to 60 video sequences from the REAL-colon dataset [3]. A vision-language model identified 1,325 candidate lesion windows spanning 22.97 hours of video. Successive verification agent filtering, AI confirmation agent with cued video from the tracking, and human review retained 528 windows (39.8%) covering 464,035 frames (12.89 hours) across 59 sequences (Table 5). The largest reduction occurred at verification filtering (422 windows removed), followed by AI confirmation (306 windows), with human review removing only 69 windows (11.6%), indicating strong agreement with automated filtering.

Curated windows average 878.9 frames compared to 414-509 for rejected ones, and carry richer annotations averaging 252.4 words per window versus 145-190 for rejected windows (Table 6). The curated set comprises 314,408 bounding boxes, 227,343 segmentation masks, and 145,515 words of clinical text (Table 4). Window duration distributions across pipeline stages are shown in Fig. 8.

### A.2 Validating the Annotations

The agentic pipeline produced 597 lesion videos, each reviewed by a clinician. Of these, 528 were accepted (88.4% success rate), totalling 464,035 frames.

We ablate each pipeline stage on the full REAL-colon dataset box annotations for polyps (Table 7, Fig. 7). Verification filtering, in which a video agent reviews the candidate window and confirms whether a lesion is present, yields the largest single-step precision gain (+7.3%) with minimal recall loss. Tracking restricts positive predictions to frames with actual bounding boxes, sharply increasing precision (+10.2%) at the cost of recall (-17.2%). AI confirmation, where a second video agent re-examines the tracked window with bounding-box overlays to validate the localised lesion, removes 34% of remaining windows and improves precision by +6.7% and F1 by +2.0pp. Human review provides a further marginal but consistent improvement (+2.4% precision, +1.0% F1), while spatial metrics remain nearly unchanged, indicating that the rejected windows had minimal impact on localisation quality.

### A.3 Colon-Bench Suite of Evaluation Benchmarks

Colon-Bench is a multi-task video benchmark for colonoscopy understanding spanning five tasks: binary lesion classification, lesion detection, instance segmentation, and visual question answering at two difficulty levels (prompted and unprompted). The benchmark comprises 1,597 unique video clips from 60 patient sequences totalling 955,126 frames (Table 9). Classification covers 790 clips (518 lesion-free, 272 lesion-positive), while detection and segmentation use the 272 and 264 lesion-positive clips respectively, providing 61,538 per-frame bounding boxes and 57,550 per-frame masks. The prompted VQA split contains 1,485 five-choice

**Table 4. Curated Colon-Bench Dataset Statistics.** Windows that passed all filtering stages (Confirmed,  $n=528$ ) are compared against those rejected during human review (Rejected,  $n=69$ ).

Metric	Confirmed (528)	Rejected (69)	Total (597)
Sequences covered	59	37	60
Total frames	464,035	28,571	492,606
Avg. frames / window	878.9	414.1	-
Duration (hours, 10 fps)	12.89	0.79	13.68
Total bounding boxes	300,132	14,276	314,408
Avg. bboxes / window	568.4	206.9	-
Bbox coverage (%)	64.7	50.0	-
Total segmentation masks	213,067	14,276	227,343
Windows with masks	465 / 528	69 / 69	534 / 597
Mask coverage (%)	45.9	50.0	-
Avg. words - initial desc.	162.8	88.6	-
Avg. words - verified desc.	55.5	53.0	-
Avg. words - confirmation note	34.2	35.7	-
Avg. words - all text combined	252.4	177.2	-
Total words (all text)	133,289	12,226	145,515

questions over 499 clips, while the unprompted split contains 2,740 questions over 918 clips and fully encompasses all detection and segmentation videos, enabling direct comparison of spatial localisation against open-ended clinical reasoning (see Table 8 for examples).

#### A.4 Benchmark Formation and Blind Tests

For each clip, three five-way multiple-choice questions are generated using Gemini 3 Flash, covering lesion identification, clinical characteristics, and temporal reasoning. The *prompted* set uses videos with bounding-box and mask overlays on confirmed lesion windows, while the *unprompted* set uses raw frames and additionally includes non-lesion windows. Both sets undergo structural validation and are randomised with a fixed seed for reproducibility. To mitigate text-only exploitability, we apply two-stage debiasing: (i) for every question, four adversarial distractors are regenerated in a separate LLM call receiving only the question stem and correct answer, producing length- and style-matched alternatives with re-randomised option positions; (ii) a blind text-only stress-test identifies cases where debiasing introduced new textual shortcuts, and these questions revert to their original formulation. After this procedure, blind-only accuracy is 44.6% (prompted) and 37.1% (unprompted) on Gemini-3 Flash versus the 20% random baseline, with residual margins attributable to skewed lesion-type distributions rather than surface-level cues (see Fig. 2).

**Table 5. Colon-Bench Filtering Funnel Overview.** Each row shows the number of windows, total frames, and video duration at successive pipeline stages. Dropped rows indicate windows removed by the corresponding filter.

Pipeline Stage	Windows	Frames	Hours	Retention (%)
VLM Detection Proposals + Merging	1,325	826,763	22.97	100.0
– Rejected by Verification Agent	–422	–178,323	–4.95	-
+ Verification Agent Filtering	903	648,440	18.01	68.2
–rejected by AI confirmation agent	–306	–155,834	–4.33	-
+ Cued AI Confirmation Agent	597	492,606	13.68	45.1
– Human Review Rejected	–69	–28,571	–0.79	-
<b>Final Curated Set</b>	<b>528</b>	<b>464,035</b>	<b>12.89</b>	<b>39.8</b>

**Table 6. Colon-Bench Annotations Stage-Wise Rejection Characteristics.** Statistics include window duration (in frames at 10 fps) and text description lengths (in words). At earlier stages, only a subset of text fields is available.

	Verification Rejected (422)	AI Confirmation Rejected (306)	Human Review Rejected (69)	Final Curated Confirmed (528)
Sequences	60	56	37	59
Total frames	178,323	155,834	28,571	464,035
Avg. frames/window	422.6	509.3	414.1	878.9
Median frames/window	339.5	417.0	259.0	599.0
Duration (hours)	4.95	4.33	0.79	12.89
<i>Text descriptions (avg. words per window)</i>				
Initial desc.	84.9	101.3	88.6	162.8
Verified desc.	60.4	53.8	53.0	55.5
Confirmation note	-	34.4	35.7	34.2
All text combined	145.3	189.5	177.2	252.4
Total words	61,326	57,976	12,226	133,289

## B Additional Results

Per-task results are reported in Tables 10 (VQA), 12 (classification), 13 (detection), and 11 (segmentation), with corresponding visualisations in Figs. 11, 12 (VQA), Fig. 14 and 15 (classification), and Fig. 13 (detection). Qualitative detection and segmentation examples are shown in Figs. 9 and 10.

**Table 7. Colon-Bench Pipeline Stage Ablation on REAL-colon [3].** Temporal metrics are frame-level detection rates. Spatial metrics (available only after tracking) report bounding-box F1 at IoU thresholds 0.25, 0.50, 0.75 and the mean IoU of matched boxes.

Pipeline Stage	Temporal (Frame-level)				Spatial (Bounding Box)			
	Prec.	Rec.	F1	Spec.	F1@.25	F1@.50	F1@.75	mIoU
VLM Detection Agent	30.9	67.5	42.4	78.6	-	-	-	-
+ Window Merging	28.9	<b>69.9</b>	40.9	75.6	-	-	-	-
+ Verification Agent Filtering	36.2	68.7	47.4	82.9	-	-	-	-
+ Spatial Localization + Tracking	46.4	51.5	48.8	91.6	<b>34.2</b>	27.7	15.1	34.4
+ AI Confirmation Agent	53.1	48.8	50.8	93.9	34.2	27.8	15.3	35.2
+ Human Review	<b>55.4</b>	48.6	<b>51.8</b>	<b>94.4</b>	34.2	<b>27.8</b>	<b>15.3</b>	<b>35.2</b>

**Table 8. Colon-Bench Example VQA Items.** Correct answers are **bolded**.

**Unprompted** (raw video; same clip as Fig. 9 / Fig. 10)

Q: How is the morphology and anatomical location of the identified lesion described?

- (A) Pedunculated polyp on a rectal fold (B) Depressed lesion on the cecal base  
 (C) Semi-pedunculated polyp in the rectum (D) **Sessile polyp on a haustral fold**  
 (E) Flat lesion on the splenic flexure

**Prompted** (video with bbox / mask overlays)

Q: At the 1.0s mark, which clinical finding is first clearly visible?

- (A) Flat mucosal lesion (Paris IIb) (B) Sessile polyp (Paris Is) (C) Subepithelial bulge  
 (D) No abnormality detected (E) **Pedunculated polyp**

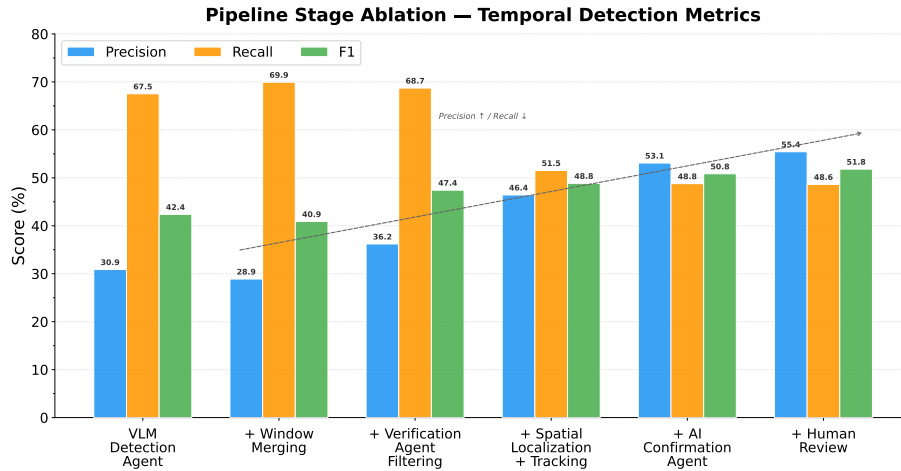


**Fig. 7. Polyp-Based Colon-Bench Pipeline Ablation.** Temporal frame-level Precision, Recall, and F1 are reported at each processing stage, from raw VLM detection through human review. Annotated values are percentages from the polyp annotations of REAL-COLON[3].

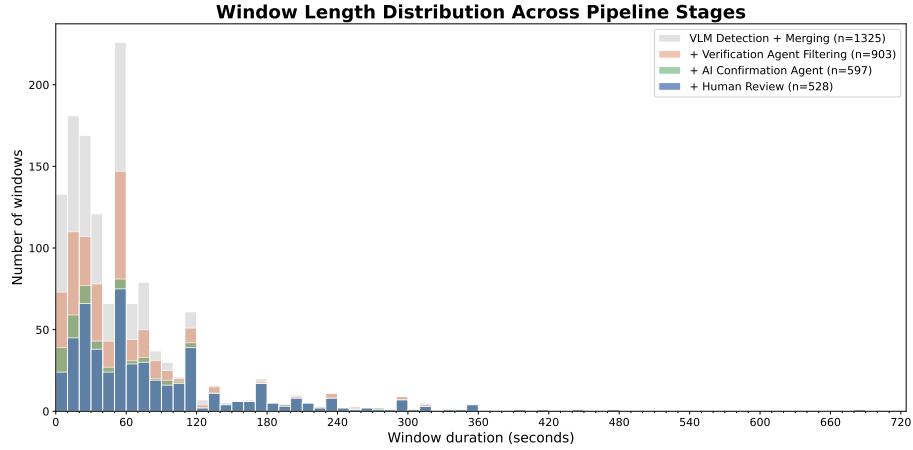


**Fig. 8. Window Duration Distributions Across Stages.** Overlaid distributions of lesion window durations (seconds at 10 FPS) are shown at successive pipeline filtering stages: VLM-detected, after verification, after AI confirmation with visual box overlays, and the final human-curated set. Each stage is a strict subset of the previous one.

**Table 9. Colon-Bench Task Statistics.** Frame counts are derived from the name mapping using per-clip start/end frame indices. Bounding boxes and masks are per-frame annotations. VQA questions are 5-choice MCQ with approximately 3 questions per video.

Statistic	Classification	Detection	Segmentation	VQA Prompted	VQA Unprompted
Total clips / questions	790	272	264	1,485	2,740
Unique videos	790	272	264	499	918
Total frames	241,996	92,311	87,631	367,572	538,115
Avg. clip length (frames)	306	339	332	737	586
Total bounding boxes	-	61,538	-	-	-
Total mask annotations	-	-	57,550	-	-
MCQ choices per question	-	-	-	5	5
Avg. questions per video	-	-	-	3.0	3.0
Unique patient sequences	60	57	57	59	60
<i>Lesion / No-lesion split</i>	272 / 518	-	-	-	-

**Table 10. Colon-Bench VQA Benchmark Accuracy.** Accuracy (%) is reported on Colon-Bench Prompted (1485 questions) and Unprompted (2740 questions), computed as correct answers divided by total questions; unanswered questions count as incorrect. Best results per benchmark are shown in **bold**.

Model	Prompted Accuracy (%)	Unprompted Accuracy (%)
Qwen3-VL 8B	32.9	38.3
Seed 1.6 Flash	38.1	45.4
Qwen-VL Max	39.1	45.4
Qwen3-VL 32B	39.3	44.4
Qwen3-VL Plus	41.2	50.5
Qwen3.5 Plus	44.3	60.5
Molmo 2-8B	46.1	53.4
Qwen3-VL 235B	46.7	56.6
Gemini 2.5 Flash Lite	47.8	46.8
Qwen3.5 397B	49.0	60.1
GLM-4.6V	55.7	53.8
Seed 1.6	62.9	72.0
Gemini 3.1 Flash Lite	69.2	67.7
Gemini 3 Flash	76.6	76.0
Gemini 3 Pro	<b>78.6</b>	<b>82.5</b>

**Table 11. Colon-Bench Segmentation Benchmark Results.** Video object segmentation results (%) are reported on the Colon-Bench segmentation benchmark (272 videos). Each model first detects the target lesion via bounding-box prompting, then a SAM-based tracker propagates the mask across the tracking window. Mean IoU and Mean Dice are computed over all evaluated frames. Best results per metric are shown in **bold**.

Model	mIoU	mDice
GPT-4o	0.5	0.8
SAM 3	2.5	2.9
Seed 1.6 Flash	2.6	3.5
Molmo 2-8B	2.6	3.8
Qwen3-VL 8B	10.4	13.1
GLM-4.6V	12.5	16.1
Seed 1.6	12.6	16.1
Qwen3-VL 32B	12.7	15.9
Qwen3-VL 235B	13.6	16.9
Claude Opus 4.6	16.1	20.5
Qwen3.5 397B	16.6	21.0
Qwen3.5 Plus	16.7	21.0
Gemini 2.5 Flash Lite	19.9	24.3
Qwen3-VL Plus	20.4	24.6
Qwen-VL Max	25.6	29.6
GPT-5.2	30.7	36.5
GPT-5.4	34.5	41.1
Gemini 3.1 Flash Lite	37.4	43.4
Gemini 3 Pro	45.0	51.3
<b>Gemini 3 Flash</b>	<b>48.3</b>	<b>54.7</b>

**Table 12. Colon-Bench Classification Benchmark Results.** Binary lesion classification results (%) are reported on the Colon-Bench classification benchmark (790 records). Each model receives a video clip and predicts whether a lesion is present (positive) or absent (negative). Accuracy is computed over all records; unevaluated records count as incorrect. Precision, Recall, and F1 are reported for the positive (lesion-present) class. Best results per metric are shown in **bold**.

Model	Acc.	Prec.	Rec.	F1
Qwen3-VL 8B	34.4	34.4	<b>100.0</b>	51.2
CLIP	34.7	34.5	<b>100.0</b>	51.3
ViCLIP	35.8	34.8	98.5	51.4
Gemini 2.5 Flash Lite	52.3	42.3	95.9	58.7
Endo-CLIP	52.9	41.9	95.2	58.2
Qwen3.5 Plus	59.1	36.2	24.6	29.3
GLM-4.6V	60.6	46.5	94.1	62.2
Colon- ViCLIP	64.4	49.0	84.2	62.0
Qwen3.5 397B	64.6	10.0	0.4	0.7
Qwen3-VL 235B	64.9	22.2	0.7	1.4
Qwen-VL Max	65.6	0.0	0.0	0.0
Qwen3-VL 32B	65.6	0.0	0.0	0.0
Qwen3-VL Plus	65.6	0.0	0.0	0.0
Molmo 2-8B	67.3	52.9	46.7	49.6
Gemini 3 Flash	72.0	55.3	97.1	70.5
Seed 1.6 Flash	72.9	<b>94.2</b>	24.3	38.6
Gemini 3 Pro	81.1	66.1	93.0	77.3
Seed 1.6	82.0	85.0	58.7	69.4
<b>Gemini 3.1 Flash Lite</b>	<b>85.1</b>	72.6	90.8	<b>80.7</b>

**Table 13. Colon-Bench Detection Benchmark Results.** Object detection results (%) are reported on the Colon-Bench detection benchmark (272 videos). Precision, Recall, and F1 are computed at  $\text{IoU} \geq 0.50$ . AP@50 is the average precision at  $\text{IoU} \geq 0.50$ ; mAP@50-95 averages AP across IoU thresholds 0.50-0.95. Mean IoU is the average intersection-over-union of matched predicted and ground-truth boxes. Best results per metric are shown in **bold**.

Model	Prec.	Rec.	F1	AP@50	mAP@50-95	mIoU
Molmo 2-8B	0.2	0.1	0.1	0.0	0.0	53.2
GPT-4o	0.6	0.1	0.2	0.0	0.0	55.4
Seed 1.6 Flash	1.6	0.5	0.8	0.0	0.0	55.7
Claude Opus 4.6	3.5	3.7	3.6	1.1	0.1	59.5
Gemini 2.5 Flash Lite	2.5	9.5	3.9	1.7	0.4	61.8
Qwen3-VL 8B	6.6	3.8	4.8	0.7	0.2	62.6
GLM-4.6V	6.6	6.2	6.4	0.5	0.1	61.6
Seed 1.6	10.4	6.6	8.0	1.1	0.2	59.7
Qwen3.5 397B	9.4	8.9	9.2	1.7	0.4	62.9
Qwen3-VL 32B	14.4	7.6	9.9	1.5	0.4	62.1
Qwen3.5 Plus	10.7	10.3	10.5	2.1	0.4	61.5
Qwen3-VL 235B	15.7	8.2	10.8	2.0	0.5	62.9
Qwen3-VL Plus	10.0	12.7	11.2	2.9	0.7	64.0
GPT-5.2	26.1	24.2	25.1	12.2	3.3	66.1
Qwen-VL Max	39.0	22.2	28.3	10.6	3.8	71.4
GPT-5.4	33.2	30.6	31.9	17.9	5.9	68.4
Gemini 3.1 Flash Lite	36.8	32.5	34.5	18.1	6.0	69.9
Gemini 3 Pro	42.2	42.5	42.3	23.7	11.1	76.3
<b>Gemini 3 Flash</b>	<b>50.9</b>	<b>52.7</b>	<b>51.8</b>	<b>32.6</b>	<b>17.0</b>	<b>79.8</b>

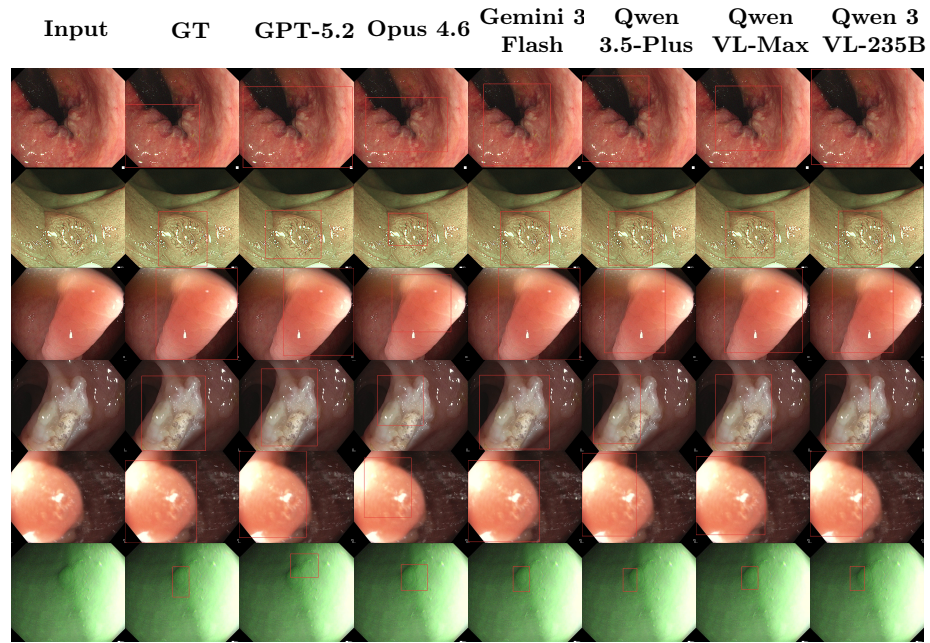


**Fig. 9. Colon-Bench Qualitative Detection Comparison.** Each row shows a different endoscopy video frame: (1) *mass*, (2) *sessile polyp*, (3) *pedunculated polyp*, (4) *ulcer*, (5) *pedunculated polyp*, (6) *sessile polyp*. Columns show the raw input, ground-truth bounding box, and predicted bounding boxes from each model. Bounding boxes are drawn in red. These detections are used in the segmentation benchmark using 3 box detections as prompts for the EdgeTAM tracker [28].

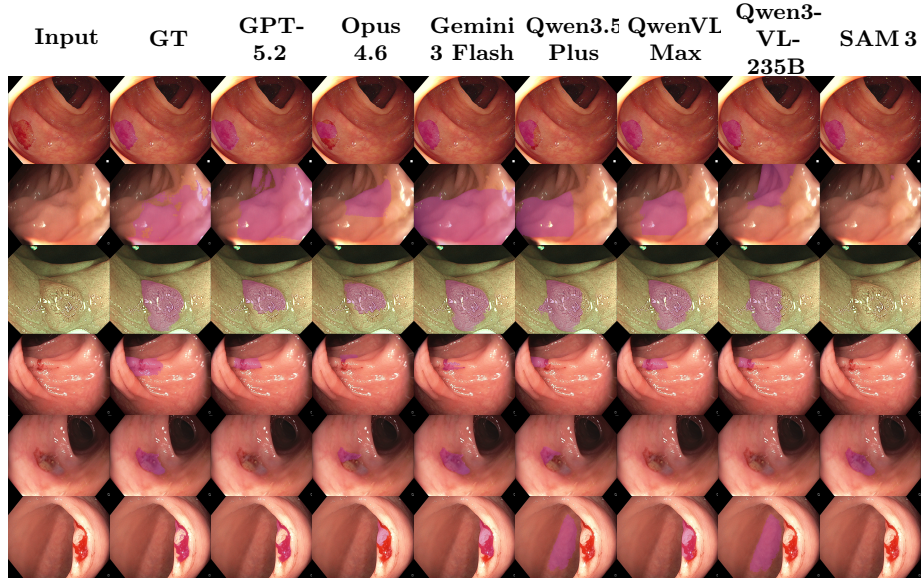


**Fig. 10. Colon-Bench Qualitative Segmentation Comparison.** Each row shows a different endoscopy video frame: (1) *erythematous region*, (2) *lipoma*, (3) *sessile polyp*, (4) *erosion*, (5) *ulcer*, (6) *erythematous region*. Columns show the raw input, ground-truth mask overlay, and predicted mask overlays from each model (including SAM3). Masks are rendered as semi-transparent purple overlays.

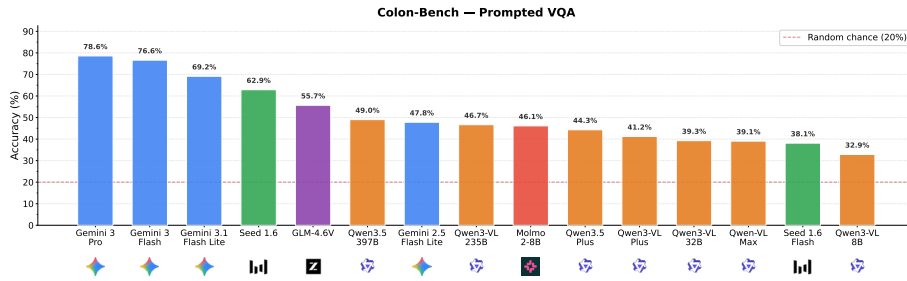


**Fig. 11. Colon-Bench Prompted VQA Accuracy.** VQA accuracy (%) on the Colon-Bench **prompted** benchmark (1,485 questions) is computed as correct answers divided by the total number of questions so that unanswered questions count as incorrect. The dashed red line indicates the 20% random-chance baseline. Models are ordered by accuracy (highest first), and colours denote model family.

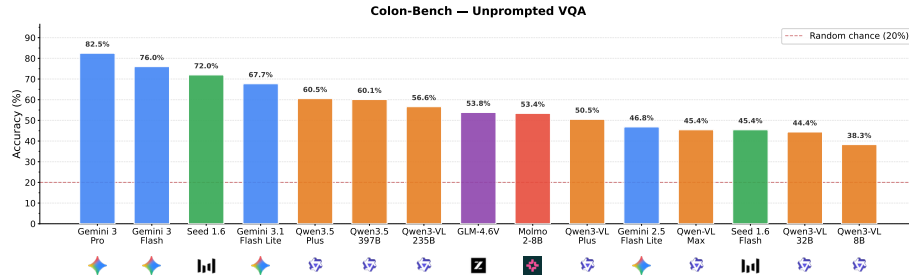


**Fig. 12. Colon-Bench Unprompted VQA Accuracy.** VQA accuracy (%) on the Colon-Bench **unprompted** benchmark (2,740 questions) follows the same protocol as the prompted benchmark: all unanswered questions are treated as incorrect. The dashed red line indicates the 20% random-chance baseline. Models are ordered by accuracy (highest first), and colours denote model family.

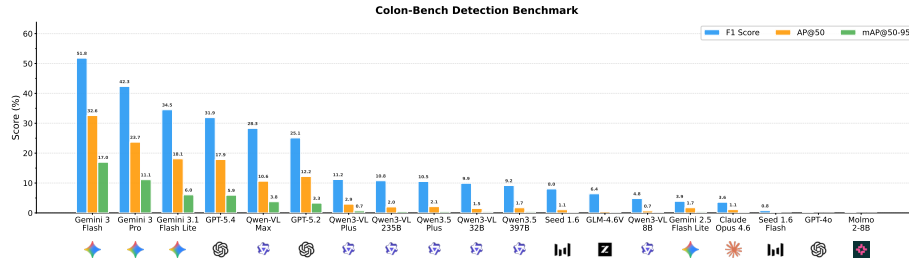


**Fig. 13. Colon-Bench Detection Metric Breakdown.** Object detection results on the Colon-Bench (272 videos) evaluate each model’s ability to localise lesions via bounding-box prediction. These detections are used in the main segmentation benchmark. Three metrics are reported for each model: **F1 Score** (primary sort key), **AP@50** (average precision at IoU  $\geq 0.50$ ), and **mAP@50-95** (mean average precision averaged over IoU thresholds 0.50-0.95). Models are ordered by F1 (highest first).

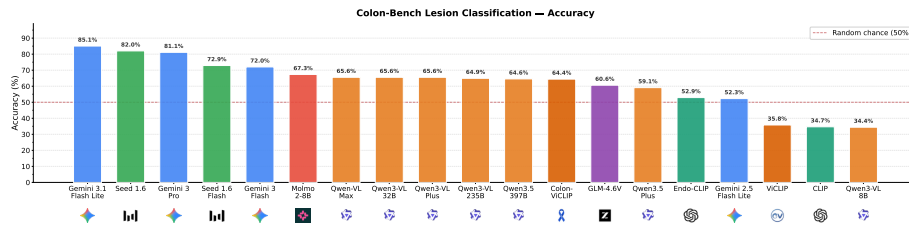


**Fig. 14. Colon-Bench Classification Accuracy Summary.** Binary lesion classification accuracy (%) on the Colon-Bench classification benchmark (790 records) is computed after each model predicts whether a lesion is present (positive) or absent (negative). Accuracy is computed over all records; unevaluated records count as incorrect. The dashed red line indicates the 50% random-chance baseline. Models are ordered by accuracy (highest first), and colours denote model family.

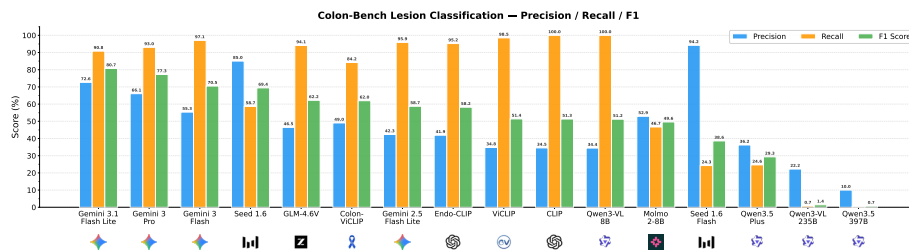


**Fig. 15. Colon-Bench Classification Precision, Recall, F1.** Binary lesion classification **Precision**, **Recall**, and **F1 Score (%)** are reported on the Colon-Bench classification benchmark (790 records) for the positive (polyp-present) class. Models are ordered by F1 (highest first).

## C Additional Analysis

### C.1 Ablation Study

We study four ablations with tabulated results in Tabs. 14-16. The detection frame count ablation shows steady gains in downstream segmentation quality, with Gemini 3 Flash improving mIoU/mDice as frames rise (Tab. 14). The temporal context ablation for binary lesion classification compares video vs. single-frame inputs and finds temporal context is generally helpful, especially for Seed 1.6, while Gemini 3 Flash is slightly stronger on frames (Tab. 17). The bounding-box annotation ablation for VQA shows only marginal changes, indicating limited dependence on explicit boxes (Tab. 15). The temporal context ablation for prompted VQA shows small, model-dependent shifts, with most models benefiting from video but a few showing minor gains on frames (Tab. 16).

**Table 14. Colon-Bench Ablation: Detection Frames for Segmentation.** Each column pair reports Mean IoU and Mean Dice for the given number of detection frames. Best results per frame count are shown in **bold**.

Model	1 Frame		2 Frames		3 Frames		5 Frames		7 Frames	
	mIoU	mDice	mIoU	mDice	mIoU	mDice	mIoU	mDice	mIoU	mDice
Seed 1.6	10.1	12.4	9.3	11.8	13.0	16.6	13.9	17.9	14.7	19.2
Qwen-VL Max	19.7	22.6	20.2	23.4	25.2	29.3	31.3	36.3	33.7	39.4
Gemini 3 Flash	43.1	48.8	46.0	52.2	49.0	55.2	53.6	60.3	54.4	61.5

**Table 15. Colon-Bench Ablation: Bounding-Box Effect on VQA.** “With bbox” uses annotated videos containing polyp bounding boxes, while “Without bbox” uses frame-generated videos of the same lesion windows without annotations (499 matched clip windows).  $\Delta = \text{Without} - \text{With}$ . Best results per condition are shown in **bold**.

Model	With bbox	W/o bbox	$\Delta$
Qwen-VL Max	39.1	37.2	-1.8
Gemini 2.5 Flash Lite	48.5	47.8	-0.7
Qwen3.5 397B	49.0	48.1	-0.9
Gemini 3 Flash	76.6	77.2	+0.6

### C.2 Colon-Skill for MLLMs

We investigate whether MLLMs benefit from structured domain knowledge at inference time. We first collect per-model VQA predictions and stratify errors by lesion category (Figs. 17 and 18), retaining questions that a majority of models

**Table 16. Colon-Bench Ablation: Temporal Context for Prompted VQA.** “Video” uses the full video clip and “Frame” uses a single representative frame over 1485 questions.  $\Delta = \text{Frame} - \text{Video}$ . Best results per condition are shown in **bold**.

Model	Video		Frame	$\Delta$
Qwen-VL Max	<b>37.5</b>	34.1	34.1	-3.4
Gemini 2.5 Flash Lite	46.7	<b>48.0</b>	48.0	+1.3
Qwen 3.5 397b	49.6	42.6	42.6	-7.0
Gemini 3 Flash	76.8	74.3	74.3	-2.5

**Table 17. Colon-Bench Ablation: Temporal Context for Classification.** “Video” uses the full video clip and “Frame” uses a single representative frame.  $\Delta = \text{Frame} - \text{Video}$ . Best results per condition are shown in **bold**.

Model	Accuracy (%)			F1 Score (%)		
	Video	Frame	$\Delta$	Video	Frame	$\Delta$
Qwen VL Max	65.6	<b>49.6</b>	-15.9	0.0	0.0	0.0
Gemini 3 Flash	69.1	70.8	+1.6	68.6	<b>69.5</b>	+0.9
Seed 1.6	82.4	60.0	-22.4	69.9	60.8	-9.1

answer incorrectly. A frontier LLM then synthesises these shared failure cases into a concise natural-language *Colon-Skill* comprising morphological cues, common confusion traps, and a decision checklist. This skill context is prepended to every VQA prompt at inference time.

Across nine MLLMs, skill-augmented prompting yields gains of up to +9.7% (prompted) and +9.0% (unprompted), with the effect most pronounced for higher-capacity models (Table 18, Figs. 19 and 20). Smaller models such as Molmo-2-8B show marginal or slightly negative deltas, suggesting sufficient model capacity is needed to integrate the additional context.

**Table 18. Colon-Skill VQA Gains.** Effect of skill-context prompting on VQA accuracy (%) across Unprompted (2740 questions) and Prompted (1485 questions) splits. Baseline uses the default prompt; With Skill appends a distilled skill context.  $\Delta$  is the absolute change in percentage points. Best results per split are shown in **bold**.

Model	Unprompted			Prompted		
	Baseline w/ Skill	Δ		Baseline w/ Skill	Δ	
Gemini 3 Flash	76.0	78.9	+3.0	76.6	78.5	+1.8
Qwen 3.5 Plus	60.5	58.6	-1.9	44.3	45.0	+0.7
Qwen 3.5 397B	60.1	63.8	+3.8	49.0	58.7	<b>+9.7</b>
Qwen 3 VL 235B	56.6	60.5	+3.9	46.7	50.1	+3.4
Molmo 2 8B	53.4	51.2	-2.2	46.1	44.4	-1.8
Qwen 3 VL Plus	50.5	56.6	+6.1	41.2	46.1	+4.9
Qwen VL Max	45.4	53.1	+7.7	39.1	40.8	+1.8
Qwen 3 VL 32B	44.4	49.6	+5.2	39.3	43.5	+4.2
Qwen 3 VL 8B	38.3	47.3	<b>+9.0</b>	32.9	38.8	+5.9

```

Colon-Skill

## Universal Anti-Error Rules

* **Do not hallucinate stalks:** The most common morphological error is calling a sessile (broad-based) polyp "pedunculated ." If the lesion sits flatly on a haustral fold without a distinct, narrowed fibrous tether, it is a sessile or flat-elevated lesion.
* **Correctly interpret NBI (Narrow-Band Imaging):** Under NBI, healthy mucosa appears greenish/cyan. Adenomas typically appear brownish with regular pit patterns, while hyperplastic or sessile serrated lesions (SSLs) appear pale or whitish. Do not confuse white-light colors with NBI colors.
* **Differentiate holes from masses:** Models consistently mistake diverticula (dark, hollow outpouchings) for depressed flat lesions or dark polyps. If a finding is a perfectly circular dark shadow with smooth margins, it is a hole/pocket, not a lesion.
* **Be conservative with size estimates:** Models routinely overestimate diminutive lesions. Without tool reference, subtle, dome-shaped nodules on folds are usually 3-5mm (diminutive). Lesions occupying a large portion of the lumen are >15 mm.
* **Accurately identify interventions:**
  * *Water jet:* Used for irrigation/clearing mucus or blood (not for coagulation).
  * *Needle catheter:* Injects fluid to create a blue submucosal cushion (lifts flat lesions).
  * *Cold/Hot Snare:* Wire loop used for Endoscopic Mucosal Resection (EMR) or polypectomy.

## Lesion Morphology Cues by Category

* **Sessile Polyps (Paris Is / Iia):** Broad base, typically situated on the crest of a haustral fold. Often pale, isochromatic (matches mucosa color), or slightly yellowish. Surface is smooth or subtly granular.
* **Sessile Serrated Lesions (SSL):** Flat, highly subtle, pale/isochromatic lesions. Key visual signatures include a "cloud-like" surface texture, indistinct/blurred borders, and a distinct "mucus cap" (adherent yellow/white debris).
* **Angioectasia / Angiodysplasia:** Sits completely flush with the mucosa. Appears as a bright, cherry-red, "fern-like" or stellate pattern of tortuous, dilated submucosal blood vessels.
* **Pedunculated Polyps (Paris Ip):** Features a distinct, thick or thin stalk attached to the colonic wall. The head is usually bulbous, multi-lobulated, and noticeably redder (erythematous) than the stalk.
* **Ulcers:** Deep or shallow punched-out depressions. Look for white/yellow necrotic slough or fibrin exudate in the center, surrounded by raised, rolled, and erythematous margins.
* **Diverticula:** Distinct, dark, circular pockets with smooth, well-defined rims. Often seen in clusters.

## Common Confusion Traps and How to Resolve Them

* **Trap: Angioectasia vs. Suction Artifact vs. Dieulafoy:** Models overwhelmingly fail here. *Resolution:* Suction artifacts are tiny, non-specific red petechial spots. Dieulafoy/ulcers involve tissue defects or active arterial spurts. Angioectasia is a flat network of "fern-like", branching dilated vessels without a mucosal defect.
* **Trap: Diverticulum vs. Depressed Lesion (Paris Iic):** *Resolution:* A diverticulum is a true anatomical hole (deep black center, hollow). A Paris Iic lesion is a mucosal depression with a visible base, often showing irregular margins and altered pit patterns.
* **Trap: Mischaracterizing pale flat lesions:** Models frequently call pale, mucus-covered flat lesions "ulcers" or "tumors." *Resolution:* If a flat lesion is pale with a "cloud-like" surface and lacks rolled margins or central necrosis, it is an SSL, not an ulcer or malignant tumor.
* **Trap: "Lobulated" vs. "Smooth" surface confusion:** *Resolution:* "Smooth" dome-shaped pale nodules are typically diminutive hyperplastic or small sessile polyps. "Lobulated" or "cerebriform" (brain-like) surfaces with redder hues indicate adenomatous polyps.
* **Trap: Mistaking anatomical folds for masses:** *Resolution:* Prominent haustral folds curve predictably around the lumen. Do not label a normal fold as a "sessile mass" unless there is a localized change in color, vascularity, or elevation (nodularity).

## Fast VQA Decision Checklist

1. **Assesses the geometry:** Is it a mass (protruding), a defect (depressed/ulcerated), a hole (diverticulum), or a flat vascular anomaly?
2. **Evaluate the attachment:** If it's a polyp, is it draped over/broadly attached to a fold (sessile) or hanging by a tether (pedunculated)?
3. **Check the lighting mode:** Is the image under white light (pink/red hues) or NBI/BLI (green/brown/cyan hues)? Adjust color descriptions accordingly.
4. **Examine the surface & margins:** Is the surface smooth, cloud-like, granular, or lobulated? Are the margins sharp, rolled, or indistinct?
5. **Identify active tools or residue:** Are there white/yellow strings (mucus/stool), active red oozing (bleeding), a wire loop (snare), or blue fluid (submucosal injection)?

```

**Fig. 16. Colon-Skill Prompt Context.** The colon-skill *SKILL.md* file is used as context augmentation for MLLMs in the VQA benchmarks. The skill is extracted by analysing error patterns across lesion categories and examples of failure modes.

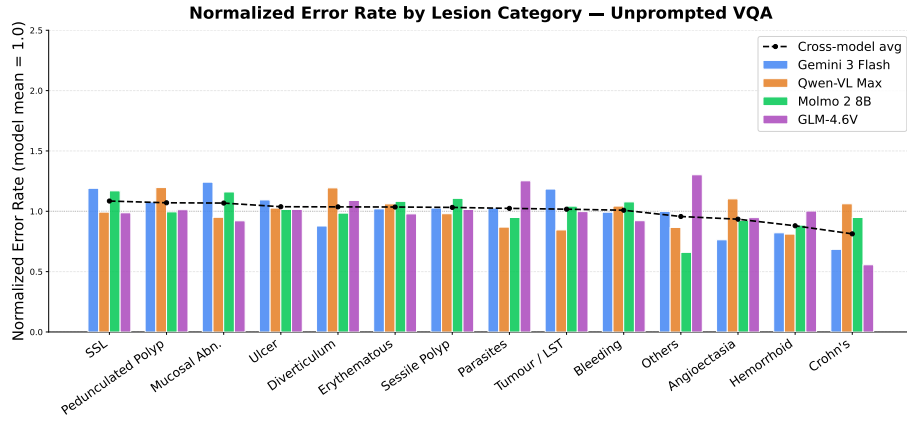


**Fig. 17. Error Patterns: Unprompted Split.** Normalized error rate by lesion category (1.0 = model average).

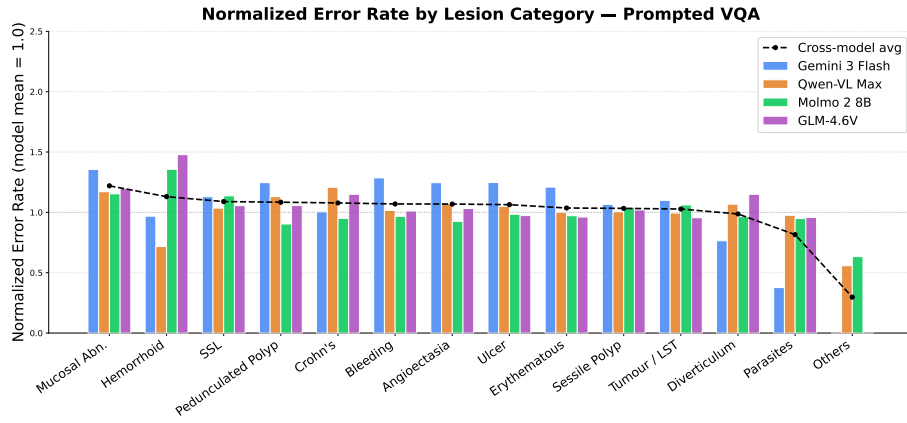


**Fig. 18. Error Patterns: Prompted Split.** Normalized error rate by lesion category (1.0 = model average).

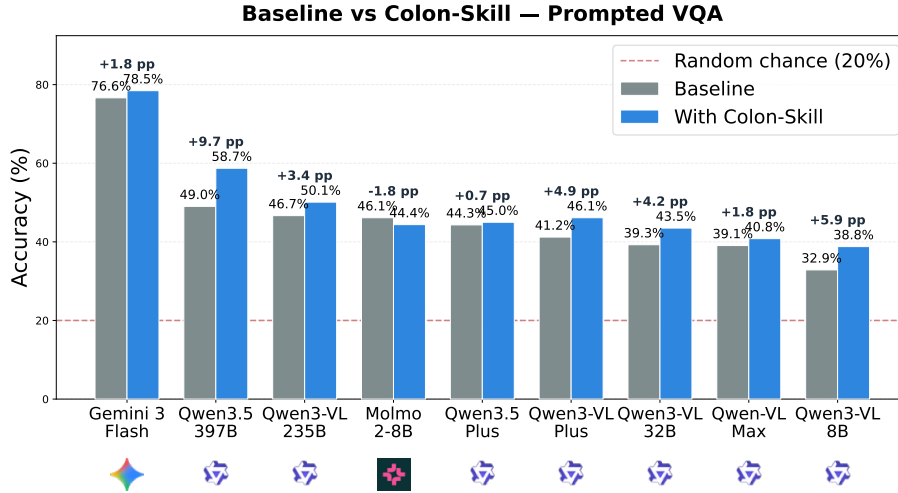


**Fig. 19. Colon-Skill Effect: Prompted VQA.** Effect of skill context on VQA performance (*prompted* split).

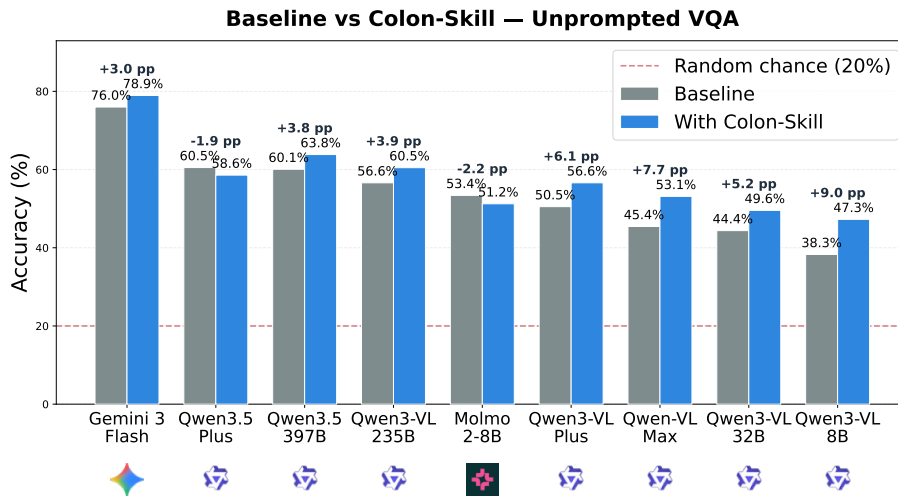


**Fig. 20. Colon-Skill Effect: Unprompted VQA.** Effect of skill context on VQA performance (*unprompted* split).